Groundwater Recharge Estimation and Salinity Risk in Magra Plain (Algeria)

Abdelmadjid Boufekane[1*], Djamel Maizi[1], Gianluigi Busico[2], Mohamed Meddi[3]

[1] Geo-Environment Laboratory, Department of Geology, Faculty of Earth Sciences and Country Planning, University of Sciences and Technology Houari Boumediene (USTHB), 16111, Algiers, Algeria.

[2] DiSTABiF - Department of Environmental, Biological and Pharmaceutical Sciences and Technologies, Campania 7 University "Luigi Vanvitelli", Via Vivaldi 43, 81100 Caserta, Italy.

[3] GEE Research Laboratory, Ecole Nationale Supérieure d'Hydraulique de Blida, 09000, Blida, Algeria.

Abstract

In this study, an approach for assessing groundwater recharge and identifying areas at risk of salinity pollution was developed in Magra Plain (Algeria). This approach is based on the hydraulic characteristics of the vadose zone, precipitation, evapotranspiration, and soil moisture, using the Hydrus-1D model. The groundwater recharge was estimated in relationship to the annual cumulative values of the soil's actual evaporation and actual transpiration, while the salinization was evaluated in relationship to the water content variation and salt dynamic in the soil profiles from September 2021 to August 2022. The results showed that the groundwater recharge of the Magra Plain varies from 3.81% to 6.19% of the total precipitation, the salinity risk of the aquifer is related to natural conditions due to climate change (temperatures, precipitation) and the thickness of a permeable layer (lithology). This modeling approach will provide an effective means of assessing the risks associated with irrigation with saline water in semi-arid regions.

Keywords: Groundwater recharge, Soil, Salinity, Hydrus-1D, Semi-arid region, Algeria.

---

* Corresponding author's email address: boufekane_ab@yahoo.fr

1. Introduction

Groundwater resources are considered the most important source of freshwater worldwide, particularly in arid and semi-arid regions, e.g. Algeria, due to the lack of water resources. Moreover, in such countries, the risk of soil and aquifer salinization is extremely increased due to the effect of climate changes on precipitation and temperature regimes, limiting the availability of drinking water (Chen et al., 2019; Panda et al., 2020). This risk becomes even higher especially in irrigation where the utilization of salty water for irrigation could exacerbate soil and groundwater salinization (Pulido-Bosch et al., 2018; Tomaz et al., 2020). So, the analysis of water salinity finalized its reduction and mitigation, and management become mandatory in many irrigated areas around the world (Ayars et al., 1999; Djoudi et al., 2023). The scenario is made even more problematic by the fact that the phenomenon of groundwater salinization could be exacerbated by anthropogenic endorheic pollution and over-exploitation of aquifers, leading to a deterioration in groundwater quality (Khezzani and Bouchemal, 2018; Mastrocicco et al., 2021).

In the aquifer system, the vadose zone can act as a filter, removing or decreasing the pollutant concentration, introduced into the subsoil such as fertilizers and pesticides (Elkayam et al., 2015; Gumiero et al., 2019; Rama et al., 2022). Moreover, the vadose media also include soil horizons where many biochemical and physical processes are responsible for pollutant degradation could occur (Amundson et al., 2007; Al-hamed et al., 2022). These depuration characteristics are mainly attributable to the high organic matter concentrations and clay contents, which can trigger pollutant biological degradation, transformation, and sorption (De Mastro et al., 2022; Ewis et al., 2022). Therefore, the vadose zone can effectively be considered a buffer zone, protecting the groundwater resources and the knowledge of its hydrogeological mandatory, so to correctly understand all the processes involved in groundwater pollution mitigation (Selker et al., 1996; Stephens, 1996).

Groundwater recharge also plays a key role in groundwater availability and quality. It is one of the main components of the hydrological cycle, and it is responsible for groundwater replenishment. Anyway, its amount greatly varies both in time and space according to several hydrogeological and climatic factors (Smerdon et al., 2010; Busico et al., 2021). In addition,

the migration and transformation of pollutants in the unsaturated zone are mainly caused by the percolation of meteoric water and accompanying physical and chemical processes like adsorption-desorption and dissolution-precipitation reactions between pollutant and soil particles (Rama et al., 2022; Xue et al., 2023).

Consequently, a proper and reliable assessment of groundwater recharge becomes mandatory to correctly estimate water resource availability and to assess aquifer vulnerability to pollutants (Scanlon et al., 2002). Many methodologies could be utilized for this purpose; the most common include water balance (Afsari et al., 2022), hydrological modeling (Razack et al., 2019), water table evolution (Boufekane et al., 2022), and natural rainfall infiltration (Ntona et al., 2022). However, changes in the piezometry and groundwater quality can be caused by many factors. Certain changes are caused by human activities (overexploitation, anthropogenic pollution) (Salifu et al. 2017; Dişli 2018), and others occur because of natural phenomena (low rainfall, high evapotranspiration) (Gain et al., 2012; Wang et al., 2022).

Among these, groundwater and solute modeling allows the understanding of all those transport processes within the unsaturated zone (Tarawneh et al., 2021). They are the methods for the analysis of different pollution scenarios, allowing the adoption of the best management actions.

Today, several models (numerical and analytical models) have been developed to assess groundwater recharge and solute transfer in the unsaturated zone, such as DAISY (Hansen et al., 1990), TOUGH2 (Pruess, 1991), SHAW (Flerchinger et al., 1996), SWAP (Van Dam et al., 1997), HYDRUS-1D (Šimůnek et al., 1998a; Šimůnek et al., 1998b), UNSATH (Fayer, 2000), and COUP (Jansson and Karlberg, 2001).

Among these, the model of Hydrus-1D (Šimůnek et al., 2005) is one of the most widely used models despite the common drawbacks of all numerical models, such as lack of input data for proper calibration and validation procedure (Ma et al., 2023; Ramos et al., 2023). The model uses two main equations for the calculation of water movement (Richards's equation, 1931) and solute transport (advection-dispersion equation, 1961) which require an iterative implicit technique (Damodhara et al., 2006). The model also allows the simulation of water, heat, and solute transport in one, two, or three-dimensional variably saturated porous media (Saâdi et al., 2018).

In this scenario, the main goals of this study are to estimate the potential groundwater recharge and the salinization risk degree for groundwater under different natural conditions

3

and to highlight the role of vadose zone buffer property for the aquifer system, using the Hydrus-1D model. Water, leaching in two soil profiles with different hydrological characteristics, will be simulated to understand how the recharge and salt concentration repond to geological and sediment characteristics. This study will offer new insight into irrigation water regulation in the Magra Plain (Algeria), providing sustainable agriculture and water development.

2. Materials and methods

2.1. Study area

The Magra plain is located in the east of M'Sila Province (Central High Plateaus of Algeria) (**Figure 1**). Three morphological units characterize the whole region: i) the Hodna Mountains, ii) the Magra Plain and iii) Soubella Valley. The area shows a flat topography with an average altitude of 567 m a.m.s.l. (Amroune, 2018) and geographically is located a few km from the Chott El Hodna (Salt Lake) and between eastern longitude 4° 49' 45" – 5° 10' 30" E and northern latitude 35° 30' 00" – 35° 40' 30" N.

The climate is classified as semi-arid with low and irregular precipitations (around 210 mm/year) and an average temperature of 19 °C for the period 1969-2015 (Amroune et al., 2020). The climatic pattern in the area is characterized by a cool dry season (spring), followed by a hot dry summer, and recently by cold and very low rainy seasons (autumn and winter). According to the Thornthwaite (1948) method and for the period 1969-2015, the evapotranspiration, runoff, and infiltration in the region are 735 mm (350%), 10 mm (5%), and 12 mm (6%), respectively. Moreover, the agricultural water deficit due to groundwater abstraction is estimated to be around 690 mm distributed throughout the year (Amroune, 2018).
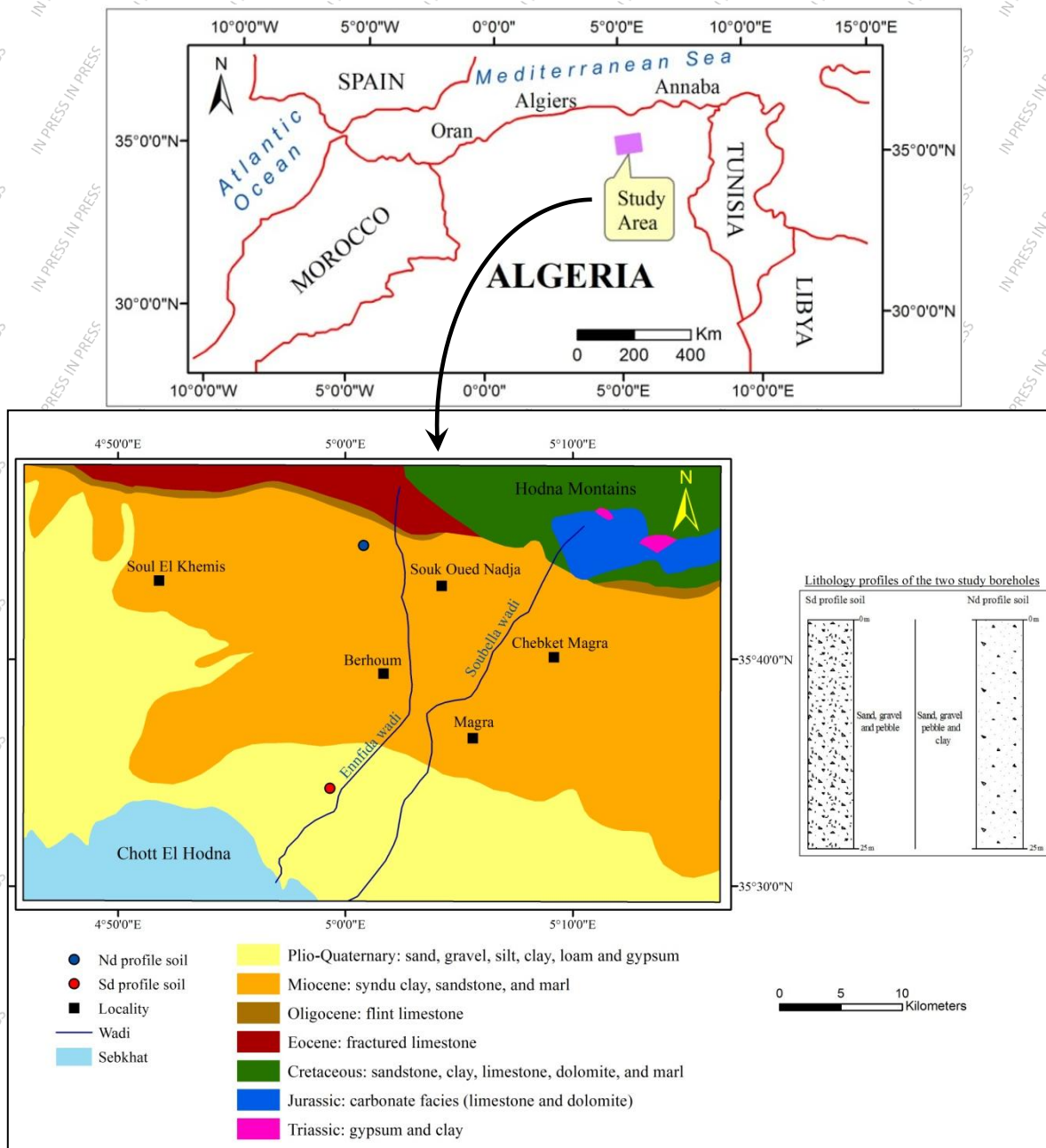
Figure 1. Location of the Magra Plain and geological map (Guiraud, 1970).

This plain is drained by two wadis (Ennfida Wadi and Soubella Wadi), flowing southward and feeding one of the largest Chott in Algeria (Chott El Hodna-Sebkhat) that are ephemeral salt lakes, present in the Saharan region of Africa.

Cereal crops, whose development and extension are highly dependent on the availability of water resources in sufficient quantity and quality, mainly represent agriculture. Groundwater is the main resource in this region.

2.2. Magra plain's soils and layers lithology

The Magra Plain is characterized by the presence of black soils derived from alluvial parent material with a clay loam or silty clay loam texture (Madani, 2023). The soils are characterized as follows:

- Mountainous area (located in the north): here the Calcaric regosols are the most diffuse soils, even though they are very little developed due to the higher slope. They have a shallow, medium to fine-grained, unconsolidated parent material, possibly alluvial in origin, and no significant soil horizon and often show accumulations of calcium carbonate or gypsum.

- Central and South area: the Isohumic soils are present and are more evolved than in the mountainous area. Moreover, approaching the Chott El Hodna (South), the soils are affected by salts.

Two profiles, belonging to the plain, were selected. The dataset of the two profiles was collected and assembled during a geotechnical study which was carried out in the area of the two profiles (Nd and Sd profiles) to a depth of 25 meters, in October-December 2021. The first is located in the northern agricultural perimeters, and the second is located in the southern part. Both profiles are characterized by direct infiltration toward the surface water table (**Figure 1**). More precisely, the Nd profile, located in the north, has a sandy-clay texture throughout its depth (25 meters). Its dry residue varies between 1 and 2 gL^{-1} (average value of 1.5 gL^{-1}). On the other hand, the Sd profile, located to the south, is marked by a sandy texture over its entire depth (25 meters). Its dry residue varies between 2 and 4 gL^{-1} (average value of 3 gL^{-1}).

2.3. Geology and Hydrogeology

According to Flandrin (1951), Bertraneu (1955), Guiraud (1969), and Sonatrach (2005) (Amroune et al., 2017), different geological formations characterize the study area and are described below chronologically (**Figure 1**).

- The Triassic formations, appearing diapirs from (gypsum and clay), outcrop in the northeast of the region.

- The Jurassic formations made of carbonate facies (limestone and dolomite) form part of the reliefs of Hodna Mountains in the northeast of the region.

- The Cretaceous formations are made of impermeable bedrock such as sandstone, clay, limestone, dolomite, and marl and form part of the reliefs of the Hodna Mountains in the northeast.

- The Eocene formations consist of fractured limestone representing the karstic aquifer in the North of the region.

- The Oligocene deposits consist of flint limestone and impermeable bedrock which characterize the North of the region.

- The Miocene deposits are essentially made of sandy clay, sandstone, and marl forming the major aquifer of the area, which occupies most of the plain.

- The Plio-Quaternary deposits are mainly formed by sand, gravel, conglomerate, silt, clay, loam, and gypsum. They represent a very productive aquifer, operated by small wells and boreholes (maximum depth: 150 meters), located in the east and south of the region.

In the southwest region, a natural outlet of the plain is observed; it is the Chott El Hodna (Sebkhat) that receives all surrounding surface waters. This Chott acts as a drainage system for water from the floods in the Magra Plain. This area also shows important salt deposits within geological formations.

Hydrogeologically, a complex multiple aquifer characterizes the study area. It is made up of two hydrogeological units:

- The first aquifer, hosted in the Eocene formations and made of fractured limestone (karstic aquifer), characterizes the north of the region.

- The second aquifer, the object of this study hosted in the Mio-Plio-Quaternary formations, is an unconfined aquifer, made of heterogeneous alluvium sediments. This aquifer represents the most important aquifer in the Magra Plain, and several wells and boreholes exploit it with depths not exceeding 80 meters.

According to the data of the National Resources Water Agency (ANRH) during the dry season of 2012, the piezometric level varies from 200 m in the South and up to 600 m in the North. The general groundwater flow is oriented from the northern side (Hodna Mountains) towards Chott El Hodna (Sebkhat) to the southwest side and it is mainly recharged for meteoric water. The large Chott (Sebkhat) is the natural outlet for groundwater.

Hydraulic conductivity varies from 2×10^{-2} to 7×10^{-2} m/s while transmissivity ranges between 5×10^{-3} and 8×10^{-3} m^2/s and aquifer thickness varies between 150 and 300 m

(Grine, 2009). However, the hydraulic gradient ranges between 2.3×10^{-3} and 8.1×10^{-3} (Grine, 2009), where the discharge water from the Hodna Mountains flows into the Magra plain, during the winter period or the flood events.

2.4. Hydrus-1D model simulation

2.4.1. Hydrus-1D model presentation

Hydrus-1D is a process-based model widely used in water and soil systems to simulate water flow, solute transport, and moisture distribution. The model was developed at California University (Šimůnek et al., 2006) to simulate the effects of irrigation on water and soil chemistry (Azhdari, 2008).

Several studies were performed worldwide, such as the United States (Šimůnek et al., 1998b; Šimůnek et al., 2005), Sweden (Gladnyeva and Saifadeen, 2012), Iran (Tafteh and Sepaskhah, 2012), China (He et al., 2017), India (Sangita et al., 2018), and Tunisia (Kanzari et al., 2018).

The Hydrus-1D model can simulate the one-dimensional water flow, heat, and solute transport in variably saturated soils (Šimůnek et al., 2006) in steady or transient regimes, using several metric systems and multiple time steps. This model is based on the Richards equation as well as the advection-dispersion equations in the case of water flow and solute transport, respectively.

Hydrus-1D solves the modified Richards' equation by eliminating the term that reflects water uptake by the roots, so that the mathematical expression for the Richards' equation will be (Šimůnek et al., 2006):

$$\frac{\partial \theta}{\partial t} = \frac{\partial}{\partial z}\left[K \left(\frac{\partial h}{\partial z} + 1 \right) \right] \qquad (1)$$

where:

h Water pressure head [L],
θ Volumetric water content [$L^3 L^{-3}$],
K unsaturated hydraulic conductivity [LT^{-1}],
t the time,
z the spatial coordinate.

The equations of Mualem and Van Genuchten (MVG) (1980) (Van Genuchten, 1980; Mualem, 1976) are used to develop the water retention curve ($\theta(h)$). The latter relates the volumetric water content in the pressure potential to the hydraulic conductivity curve ($K(h)$), as a function of its saturation state measured by h. The retention curve represented by the equation of van Genuchten (1980) is:

$$\theta(h) = \begin{array}{ll} \theta_r + \dfrac{\theta_s - \theta_r}{1 + |\alpha h^n|^m} & h < 0 \\ \theta_s & h \geq 0 \end{array} \quad \text{Where:} m = 1 - \frac{1}{n}, n > 1 \qquad (2)$$

Where:

θ_r is the residual water content [$L^3 L^{-3}$],

θ_s is the saturated water content [$L^3 L^{-3}$],

h is the water pressure head [L],

α [L^{-1}] and n are shape parameters.

The MVG equation where used for describing the hydraulic conductivity is:

$$K(h) = \begin{array}{ll} K_s r S_e^{1/2} \left[1 - \left(1 - S_e^{1/m} \right)^n \right]^2 & h < 0 \\ K_s & h \geq 0 \end{array} \qquad (3)$$

With:

$m = 1 - \frac{1}{n}$ $n > 1$ and $S_e = \frac{\theta - \theta_r}{\theta_s - \theta_r}$,

K_s the saturated hydraulic conductivity [LT^{-1}],

S_e the effective saturation [-],

r the pore connectivity parameter [-] equal to 0.5.

The equation that governs the solute transport in a variably saturated soil is the advection-dispersion equation, defined in Hydrus-1D as:

$$\frac{\partial \rho S}{\partial t} + \frac{\partial \theta C}{\partial t} = \frac{\partial}{\partial z} \left\{ \theta. D \frac{\partial C}{\partial z} \right\} - q \frac{\partial C}{\partial z} \qquad (4)$$

Where:

z the spatial coordinate,

C and S solute concentrations in the liquid [ML^{-3}] and solid [MM^{-1}] phases,

9

$S = KdC$ where Kd [L^3M^{-1}] the partition coefficient,

q the volumetric flux density [LT^{-1}],

D the dispersion coefficient [L^2T^{-1}],

ρ the bulk soil density [ML^{-3}].

2.4.2. Boundary and initial conditions

The initial condition along with boundary conditions were considered a 25 m deep vertical soil profile:

- In the case of the solute transport, the boundary conditions were coincident with the observed values of groundwater salinity.

- In the case of recharge, the upper boundary coincides with the atmospheric limit condition with surface runoff, whereas the lower boundary condition has been taken as free drainage.

At the soil surface, the reference evapotranspiration was calculated via the Penman-Monteith model, with the daily values of maximum and minimum temperature, precipitation, average humidity, and wind speed.

The Van Genuchten hydraulic parameters (θ_r, θ_s, α, n, and K_s), were calculated using the evaporation method and the hydraulic parameter values were calculated in the calibration phase.

The lower boundary condition corresponds to deep drainage where the release rate q (n), at the base of the soil profile at node n is considered as a component of the water table position (Hopmans and Stricker, 1989):

$$q(n) = q(h) = -A_{qh}\exp(B_{qh}|h - GWL0L|) \qquad (5)$$

With:

$q(h)$ is the discharge rate [cm day^{-1}],

h is the pressure head at the bottom of the soil profile [cm],

A_{qh} and B_{qh} are empirical parameters in [cm day^{-1}] and [cm^{-1}] respectively,

GWL0L is the reference groundwater depth [cm].

Vertical drainage across the lower boundary of the soil profile, in this case, is approximated by a flux that depends on the water table level.

The rate for each year daily and a total period of two years (2016-2022) was simulated. The simulation for the total period corresponds to the period between the occurrence of the first and the last rainfall event of the considered year.

2.4.3. Climate data

Data period six years from the M'Sila meteorological station were collected (from 1 September 2016 to 31 August 2022). **Figures 2**, **3,** and **4** show the data, used in the Penman-Monteith model: monthly variations of rainfall data, average values of maximum and minimum temperatures, average wind speed, and humidity, respectively.
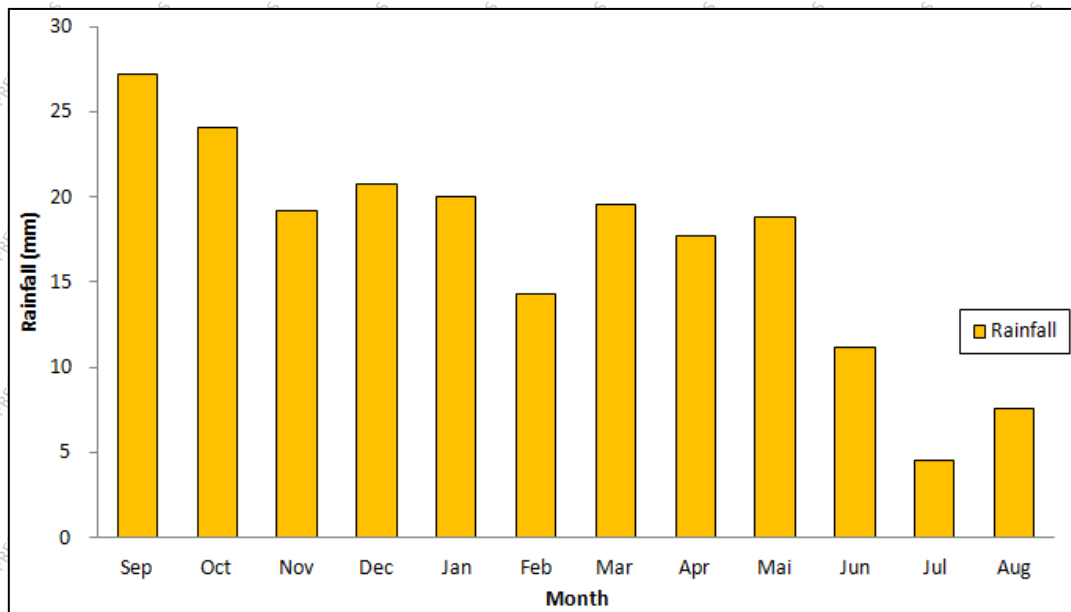
Figure 2. Average rainfall variations during the period September 2016 to August 2022.
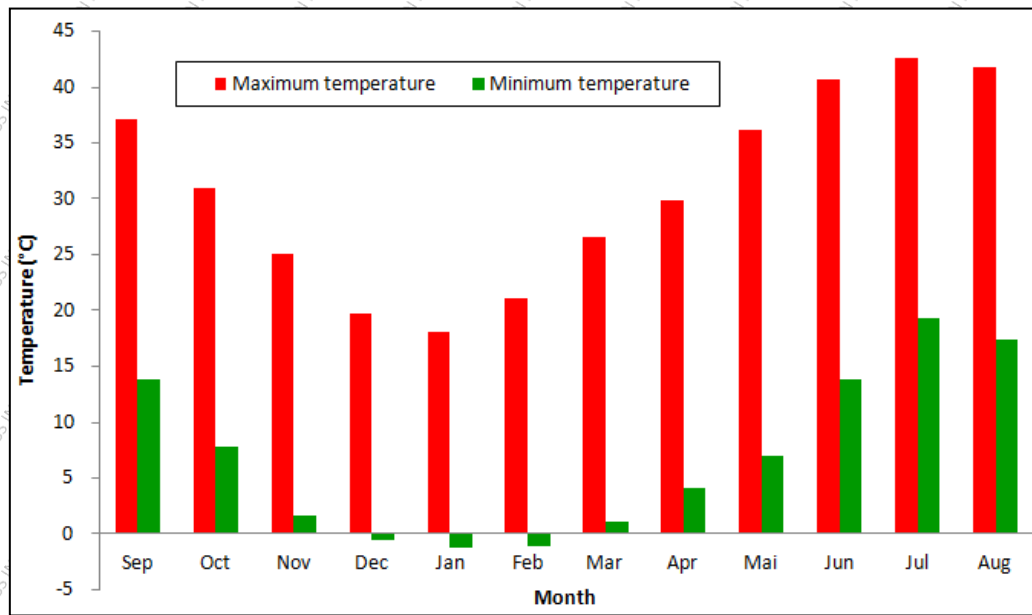
Figure 3. Daily average values of maximum and minimum temperatures during the period September 2016 to August 2022.
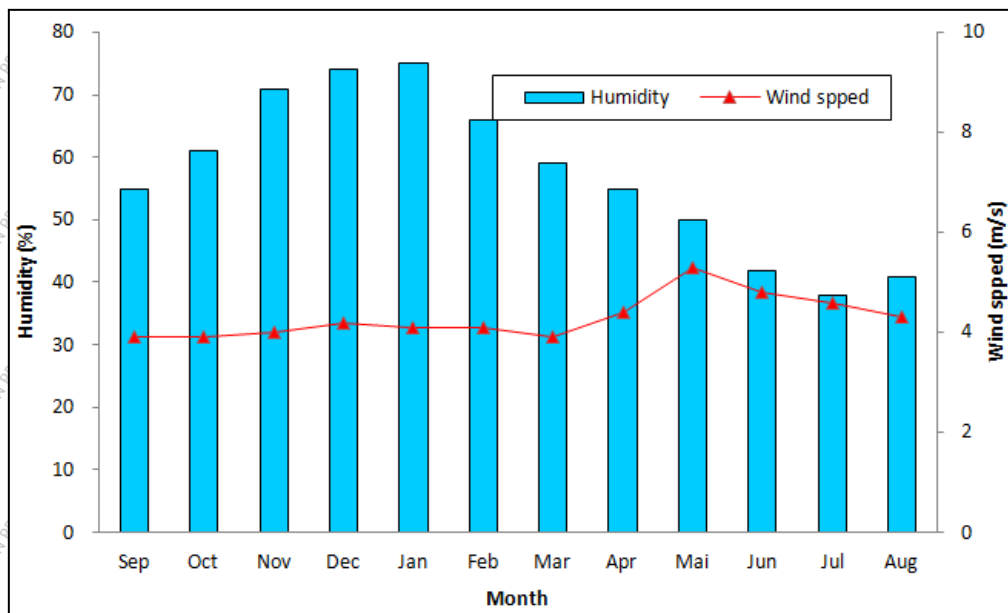
Figure 4. Average wind speed and humidity during the period September 2016 to August 2022.

2.4.4. Groundwater recharge

The main results, estimated by Hydrus-1D, are actual soil evaporation, actual transpiration, and groundwater recharge. The simulated piezometric level is assumed to be at a depth where the pressure head (h) is equal to 0. The assumption of a 1:1 gradient between h

(pressure head) and z (soil depth) was checked to be valid for the present simulations
(Leterme et al., 2012).

2.4.5. Hydrus-1D input parameters

The Rosetta model was used to define the soil hydraulic parameters (Schaap et al., 2001).
The factors of the water flow, i) saturated water content (θ_s), ii) residual water content (θ_r), iii)
inverse of the air entry value (α), iv) pore size distribution index (n), v) saturated hydraulic
conductivity (K_s), vi) the pore connectivity parameter for two different soil layers, were calculated
using the soil texture and the measured bulk density. The core sampling method was used to determine
the bulk density. The international pipette method was considered for the particle size distribution.

The calibration process allowed the estimation of soil hydraulic parameter values. In this
study, the simulations were conducted for 730 days with a daily scale. It was carried out on
silty and sandy soils that can be considered representative of the study area. For solute
transport parameters, concentration flux was used as both the upper and the lower boundary
conditions; it is calculated in the laboratory. **Table 1** presents the soil hydraulic parameters,
the Geometry information, and the solute transfer properties.

Table 1. Input parameters of Nd and Sd profiles.

Parameters	Values	
	Nd profile	Sd profile
Geometry information		
Depth (m)	25	25
Number of layers	1	1
Time information		
Simulation time (days)	730	730
Hydraulic properties		
Layers (m)	0 – 25	0 – 25
θ_r (cm^{3}cm^{-3})	0.065	0.075
θ_s (cm^{3}cm^{-3})	0.42	0.54
α(cm^{-1})	0.07	0.75
n($-$)	0.51	0.89
K_s (cm.d^{-1})	1.60	2.46
L	0.5	0.5
Solute transfer properties		
Layer (m)	0 – 25	0 – 25
Dispersion coefficient [L]	19	25
K_d[M^{-1} L^3]	0	0

Moreover, the observed values of groundwater salinity show the following:

13

- For the Nd profile: the minimum and maximum values of water content were set to ($\theta = 0.1$ cm^3cm^{-3}) and ($\theta = 0.3 \ cm^3cm^{-3}$), respectively. The average value of dry residue is C = 1.5 g/L.

- For the Sd profile: the minimum and maximum values of water content taken were set to ($\theta = 0.1 \ cm^3cm^{-3}$) and ($\theta = 0.3 \ cm^3cm^{-3}$), respectively. The average value of dry residue is C= 3 g/L.

To resume, four different combinations in the model , representing different soil water contents and salt concentrations, were used to define the initial conditions (**Table 2**).

Table 2. Initial conditions of water content and solute concentration for Nd and Sd profiles.

Profiles	Nd profile		Sd profile	
Salt concentrations: C (gL^{-1})	1.5		3.0	
Water contents: θ (cm^{3}cm^{-3})	0.1	0.3	0.1	0.3

2.5. *Model calibration and validation*

The robustness of the model was checked, using two approaches: graphical and statistical methods. For the first approach, measured and simulated volumetric water contents, groundwater recharge, and soil salinities were shown as a function of soil depth for the different time steps. The second approach is based on the calculation of the root mean square error (RMSE):

$$\text{RMSE} = \sqrt{\frac{\sum_{i=1}^{n}(p_i - m_i)^2}{n}} \ X \ \frac{1}{\bar{m}} \ X \ 100 \qquad (6)$$

Where: n is the number of observations, m_i are the measured values, p_i are the predicted values, and $\bar{m}$ is the average value of observed data.

The model was initialized for 730 days. The results of soil water and salt content were obtained at the 183th, 365th, 548th, and 730th days of simulation.

3. Results and discussion

3.1. Variations in water and salt content

3.1.1. Water content variation

According to the obtained results during the simulation period (730 days), the results of the simulation for the Nd profile are shown in **Figure 5**. In this case, the water content values vary between 0.110 cm^3cm^{-3} and 0.150 cm^3cm^{-3} at the ground surface: it slightly increases from 0 to 15 m while from 15 m to the bottom of the profile. It remains almost constant from 0.147 to 0.178 cm^3cm^{-3}. However, the simulated water content values are always lower than the initial conditions, highlighting the continuous dewatering of the unsaturated zone due to the existence of a layer of low permeability (clay layer) for the entire soil profile.

Figure 6 shows the result for the Sd profile where the water content values vary between 0.130 cm^3cm^{-3} and 0.170 cm^3cm^{-3} at the ground surface, showing progressively increases accordingly with the soil depth (bottom of the profile) varying between 0.207 and 0.265 cm^3cm^{-3}.

Contrary to the Nd simulation, the Sd profile showed higher values of water content exceeding the initial conditions in some cases. This is probability due to the permeable nature of this soil (i.e.: sandy layer) which allows a greater infiltration of water after rain events.
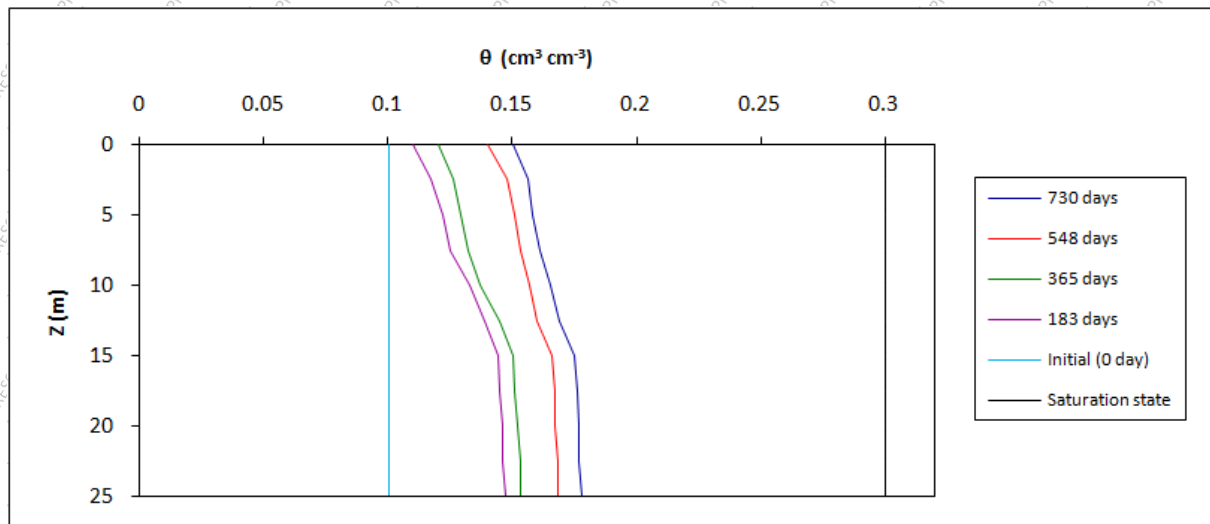
Figure 5. Variation of the water content for the Nd profile, for 730 days.
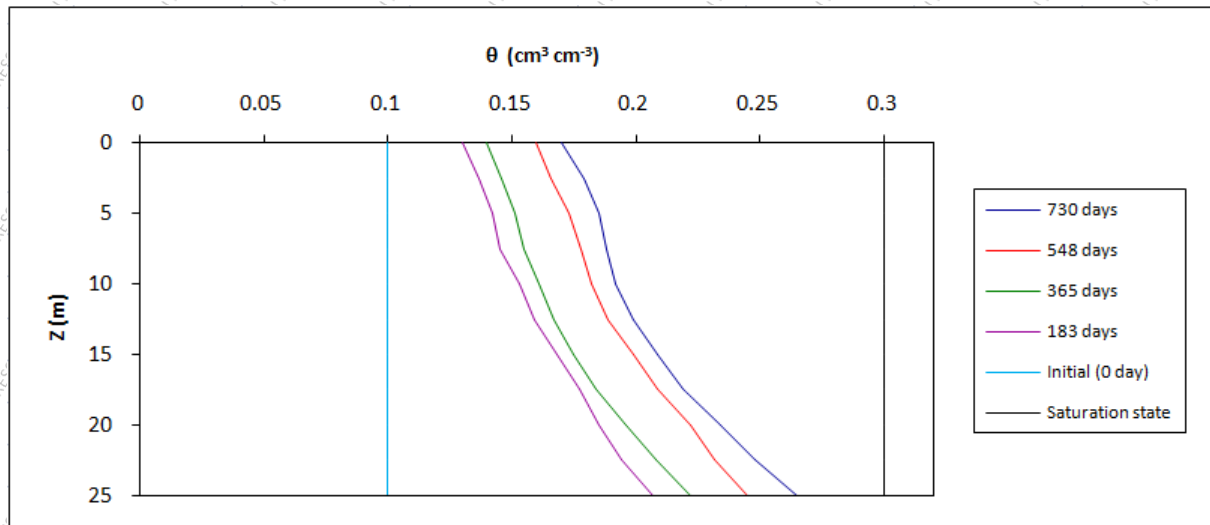
Figure 6. Variation of the water content for the Sd profile, for 730 days.

3.2.2. Salts content variation

As for the water content, the salt concentration trends obtained during the simulation period (730 days) showed similar results for all the combinations. According to the results shown in **Figure 7**, for the Nd profile, the concentration rate varies between 0.05 gL^{-1} and 0.25gL^{-1} at the ground surface. Moreover, it constantly increases until 0.69 gL^{-1} moving downward remaining constant in the last 5 meters (from 15 m to 25 m, the bottom of the profile) where the final value is 0.72 gL^{-1} after 730 days.

A general reduction in soil salinity, compared to the initial conditions (0.72 gL^{-1}), was shown when simulating the salt content profiles. A continuous leaching of salt is noticed through the unsaturated zone due to the presence of clayey intercalations that are able to slow down the spread of salt. These results highlighted the general low contamination risk for groundwater located below this kind of soil.

According to the results, shown in **Figure 8**, for the Sd profile, the concentration rate ranged between 0.32 gL^{-1} and 0.65 gL^{-1} at the ground surface. It constantly increases from 0.51 gL^{-1} to 0.94 gL^{-1} from 0 to 15 m and from 15 m to 25 m (bottom of the profile). The trends of the profile change and gradually increase towards the final salt concentration of 1.87 gL^{-1} after 730 days.

During the simulation period and under the initial conditions, the results of the variation of the solute concentration profiles showed the risk of high groundwater salinity in the area where the Sd profile is located. This can be explained by the presence of the sandy layer, which accelerates salt leaching into the aquifer and increases the salinity risk.

16
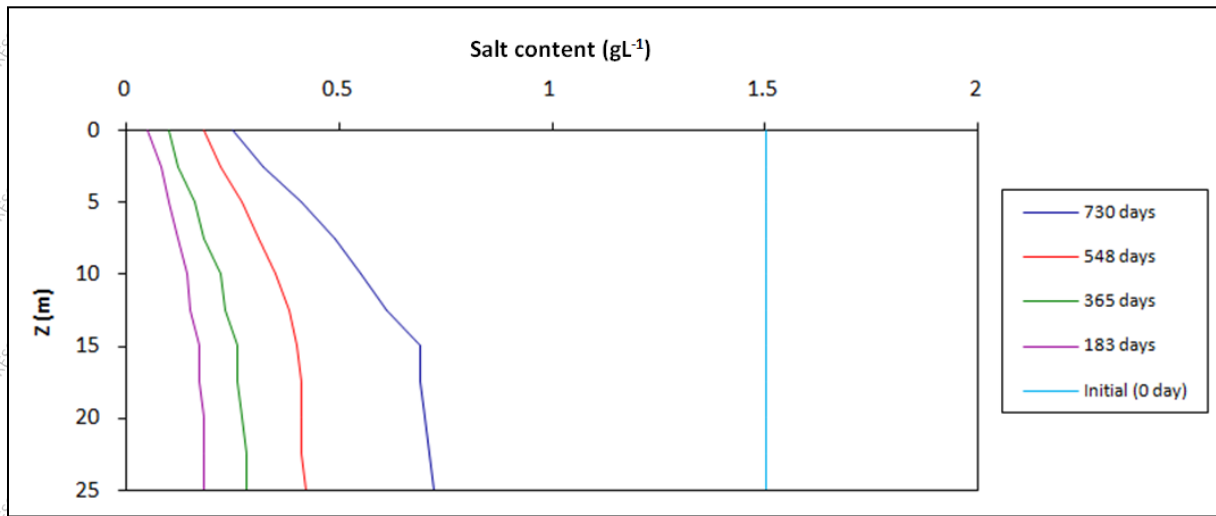
Figure 7. Variation of the salt content for the Nd profile, C = 1.5 gL^{-1}, for 730 days.
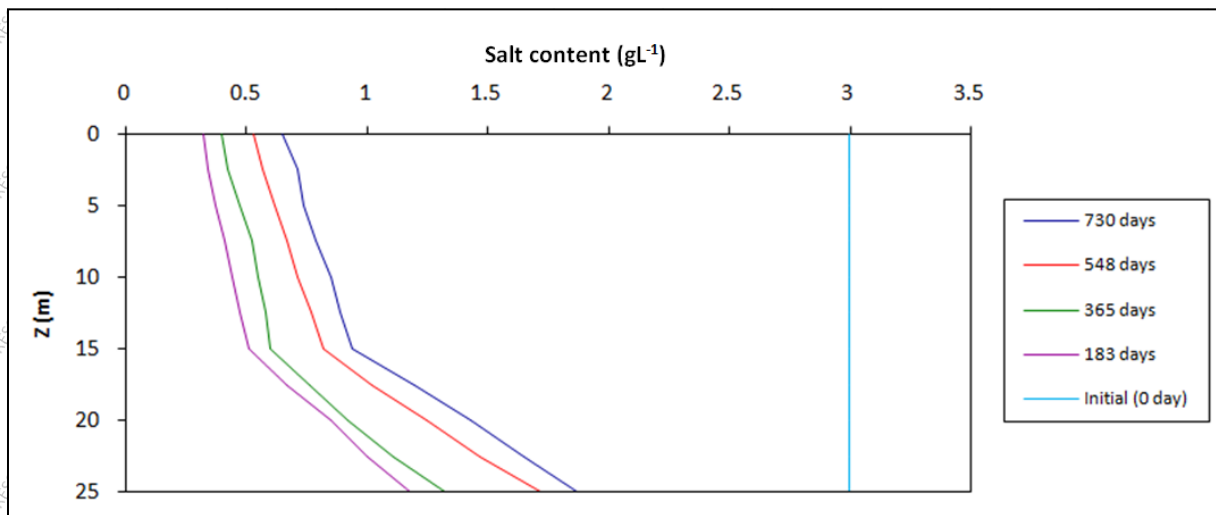
Figure 8. Variation of the salt content for the Sd profile, C = 3.0 gL^{-1}, for 730 days.

3.2.3. The calibration results of the Hydrus-1D model

The results of soil water and salt content were obtained at the 183th, 365th, 548th and 730th days of the simulation were presented in **Table 3** where the proposed model (Hydrus-1D) shows better performance in the prediction of soil water and salt content (the RMSE values are equal to 0).

Table 3. Statistical evaluation (RMSE values) of the simulation results

	Nd profile			**Sd profile**		
	RMSE			RMSE		
	WCV	SCV (1.5 gL^{-1})	SCV (3.0 gL^{-1})	WCV	SCV (1.5 gL^{-1})	SCV (3.0 gL^{-1})

183th days of simulation	0.0723	0.1234	0.1154	0.0815	0.1272	0.1306
365th days of simulation	0.0739	0.1265	0.1183	0.0826	0.1298	0.1327
548th days of simulation	0.0754	0.1291	0.1211	0.0835	0.1316	0.1350
730th days of simulation	0.0776	0.1304	0.1238	0.0842	0.1332	0.1379

WCV: Water Content Variation
SCV: Salt Content Variation

3.3. Modeling of the groundwater recharge

The Hydrus- 1D model was used to estimate the potential groundwater recharge in the study area for the period September 2021 to August 2022. Based on the research results of Leterme et al. (2012), the model was used to simulate groundwater recharge in relation to annual values of actual soil evaporation and transpiration. The Penman-Monteith model was used to calculate intercepted water evaporation, potential soil evaporation, and potential transpiration. These variables will be used in the Hydrus-1D model.

In the current simulation, the results (**Tables 4 and 5**) show, that in the North zone of the plain (Nd profile), the simulated groundwater recharge is equal to an average of 8 mm/yr coincident with the 3.81% of total rainfall, while the actual ET (ETa) is 93.24% of the potential ET (ET0). For the south zone of the plain instead), (Sd profile) the simulated actual groundwater recharge is around 13 mm/yr (6.19% of total rainfall), and the actual ET (ETa) is 94.42% of the potential ET (ET0).

Table 4. Average values of rainfall, potential groundwater recharge, potential actual evapotranspiration and potential reference evapotranspiration during the period September 2021 to August 2022.

Zones of the plain	Rainfall (R)	Potential Groundwater recharge (GR)	Potential actual evapotranspiration (ETa)	Potential reference evapotranspiration (ET0)
		mm/yr		
North zone (Nd profile)	210	8	1021	1095
South zone (Sd profile)	210	13	1068	1131

Figure 9 shows the potential groundwater recharge for the two soil profiles Nd and Sd during the period September 2021 to August 2022. The Magra plain is characterized by low annual precipitation (210 mm), and groundwater recharge shows almost no seasonality. The average groundwater depth, used for the numerical simulations, is 10 mm (8 to 13 mm). The higher monthly recharge was obtained in December, January, February, and March. According to these recharge values, it concluded that the monthly groundwater recharge values are related to the monthly climatic parameters (precipitation, temperature, and evaporation) (Boufekane et al., 2019) and to the lithology of the unsaturated zone (permeable or impermeable layer) (Boufekane et al., 2022).
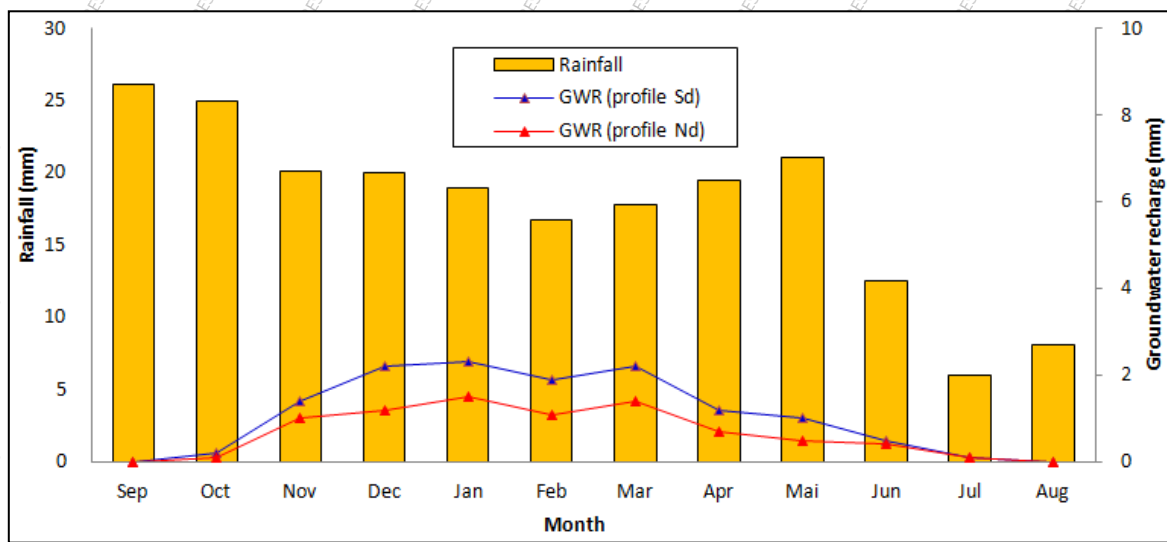
Figure 9. Potential groundwater recharge from two profiles soils during the period September 2021 to August 2022.

Table 5. Average monthly values of simulated potential groundwater recharge during the period September 2021 to August 2022.

Month	Potential Groundwater recharge (mm)												Total Year
	Sep	Oct	Nov	Dec	Jan	Feb	Mar	Apr	Mai	Jun	Jul	Aug	
Nd profile	0	0.1	1.0	1.2	1.5	1.1	1.4	0.7	0.5	0.4	0.1	0	**8.0**
Sd profile	0	0.2	1.4	2.2	2.3	1.9	2.2	1.2	1.0	0.5	0.1	0	**13.0**

In this semi-arid region, low-intensity rainfall does not play a very important role in groundwater recharge via infiltration and a considerable proportion of the precipitated water is lost via evaporation. Therefore, only torrential rains are capable of contributing to the groundwater supply.

The results of the simulation indicated that soil characteristics have a significant effect on soil water storage, and that the increasing use of irrigation amount could accelerate salt leaching as already stated also in different environments such as China (Zeng et al., 2014). Moreover, irrigation in agriculture significantly alters the water cycle, often with major environmental consequences, by increasing the salinity of recharge water from irrigated permeable soils and by recharging unconfined aquifers in drier regions such as Spain and South America (Foster et al., 2018).

4. Conclusion

In semi-arid regions like the Magra Plain (Algeria), salinization of groundwater due to intrinsic climatic characteristics, is a worrying issue to be managed and resolved. This study examined the interactions between the aquifer and the vadose zone to assess groundwater recharge and salinity risk. The main factors, influencing groundwater recharge salinity risk, are: rainfall, evaporation, soil nature, and vegetation.

The Hydrus-1D model was applied in the Magra plain. In the absence of soil layer information, except for texture, the approach, using combinations of initial conditions, is effective for predicting groundwater quality in the case of direct recharge. The results highlighted that the sandy layer accelerates infiltration towards the depths as well as the influence of water dynamics in the vadose zone. Conversely, the existence of clay intercalations in the unsaturated zone slows down the transit of water towards the aquifer (providing a good protection for groundwater). The sandy layer increases the salinity risk to the aquifer while the existence of clay intercalations in the unsaturated zone protects the aquifer against the filtrations of pollutants towards the groundwater. The recharge estimated during the period September 2021 to August 2022 varied from 8 to 13 mm (3.81% to 6.19% of total rainfall). The highest potential recharge was found for sandy clay and the lowest one for sandy soils. In addition, the decline in rainfall, the increase in temperature and evaporation will continue to threaten the groundwater resources (quantity and quality).

Finally, according to Hydrus-1D model results, as recommendations to improve this study, additional scenarios, including multi-factorial analysis study of rainfall, evaporation and groundwater recharge, and longer-term simulations, need to be considered to increase results reliability. Moreover, this elaboration can give useful insight to minimize the risks of groundwater overexploitation and salinity, especially, in arid and semi-arid regions.

References

Afsari, N., Murshed, S. B., Uddin, S. M. N., and Hasan, M. (2022). Opportunities and Barriers Against Successive Implementation of Rainwater Harvesting Options to Ensure Water Security in Southwestern Coastal Region of Bangladesh. Front. Water 4: 811918. https://doi: 10.3389/frwa.2022.811918

Al-hamed, T., Shiyab, S.M., Al-Bakri, J. (2022). Morpho-physiological Effects of Drought on Medicinal Plants and the Potential Use of Remote Sensing - A Review. Jordan Journal of Earth and Environmental Sciences 13(2): 105-113. https://jjees.hu.edu.jo/files/Vol13No2/JJEES_Vol_13_No_2_P5.pdf

Amroune, A. (2018). Study of the hydrochemical contribution in the functioning knowledge of the alluvial aquifer in the northern region of Hodna (South-East Algeria). PhD thesis, University of Batna 2, Batna, Algeria. http://theses.univ-batna.dz

Amroune, A., Boudoukha, A., Boumazbeur, A., Benaabidate, L., Guastaldi, E. (2017). Groundwater geochemistry and environmental isotopes of the Hodna area, Southeastern Algeria. Desalination and Water Treatment 73: 225-236. https://doi.org/10.5004/dwt.2017.20642

Amroune, A., Mihoub, R., Enrico, G., Urena-Nieto Carlos U.N. (2020). Groundwater flow dynamics and distribution of hydrochemical facies using GIS in Hodna plain, M'Sila, southeastern Algeria. International Journal of Sustainable Development and Planning 15(6): 789-800. https://doi.org/10.18280/ijsdp.150601

Amundson, R., Richter, D.D., Humphreys, G.S., Jobbágy, E.G., Gaillardet, J. (2007). Coupling between biota and earth materials in the critical zone. Elements 3: 327-332. https://doi.org/10.2113/gselements.3.5.327

Ayars, J.E., Tanji, K.K. (1999). Effects of drainage on water quality in arid and semiarid lands. In: Skaggs RW, Van Schilfgaarde J (eds) Agricultural drainage. ASA-CSSA-SSSA, Madison, pp 831-867. https://doi.org/10.2134/agronmonogr38.c25

Azhdari, K. (2008). Simulation of moisture distribution in soil in drip irrigation system using HYDRUS2D model. Journal of agricultural sciences and natural resources 15: 168-180.

Boufekane, A., Saibi, H., Benlaoukli, B., Saighi, O. (2019). Scenario modeling of the groundwater in a coastal aquifer (Jijel plain area, Algeria). Arabian Journal of Geosciences 12: 799. https://doi.org/10.1007/s12517-019-4965-0

Boufekane, A., Maizi, D., Madene, E., Busico, G., Zghibi, A. (2022). Hybridization of GALDIT method to assess actual and future coastal vulnerability to seawater intrusion. Journal of Environmental management 218: 115580. https://doi.org/10.1016/j.jenvman.2022.115580

Busico, G., Ntona, M.M., Carvalho, S. C. P., Patrikaki, O., Voudouris, K., Kazakis, N. (2021). Simulating future groundwater recharge in coastal and inland catchments. Water Resources Management 35(11): 3617-3632. https://doi.org/10.1007/s11269-021-02907-2

Chen, Y., Vigouroux, G., Bring, A., Cvetković, V., Destouni, G. (2019). Dominant hydro-climatic drivers of water temperature, salinity, and flow variability for the large-scale system of the Baltic Coastal Wetlands. Water 11(3): 552. https://doi.org/10.3390/w11030552

Damodhara, R.M., Raghuwanshi, N.S., Singh, R. (2006). Development of a physically based 1d-infiltration model for irrigated soils. Agricultural Water Management 85: 165-174. https://doi.org/10.1016/j.agwat.2006.04.009

De Mastro, F., Cacace, C., Traversa, A., Pallara, M., Cocozza, C., Mottola, F., Brunetti G. (2022). Influence of chemical and mineralogical soil properties on the adsorption of sulfamethoxazole and diclofenac in Mediterranean soils. Chemical and Biological Technologies in agriculture 9: 34. https://doi.org/10.1186/s40538-022-00300-8

Dişli E. (2018) Evaluation of hydrogeochemical processes for waters' chemical composition and stable isotope investigation of groundwater/surface water in karst-dominated terrain. Aquatic Geochemistry, The Upper Tigris River Basin, Turkey. https:// doi. org/ 10.1007/ s10498- 019- 09349-8

Djoudi, S., Pistre, S., Houha, B. (2023). Evaluation of Groundwater Quality and its Suitability for Drinking and Agricultural Use in F'kirina Plain, Northern Algeria. Jordan Journal of Earth and Environmental Sciences 14(3): 203-209. https://jjees.hu.edu.jo/files/Vol14/No.3/JJEES_Vol_14_No_3_P4.pdf

Elkayam, R.,Sopliniak, A., Gasser, G.,Pankratov, I., Lev, O. (2015). Oxidizer demand in the unsaturated zone of a surface-spreading Soil Aquifer Treatment system. Vadose Zone Journal 14: 11. https://doi.org/10.2136/vzj2015.03.0047

Ewis, D., Ba-Abbad, M.M., Benamor, A., Muftah H. El-Naas, M.H. (2022). Adsorption of organic water pollutants by clays and clay minerals composites: A comprehensive review. Applied Clay Science 229: 106686. https://doi.org/10.1016/j.clay.2022.106686

Fayer, M.J. (2000). UNSAT-H version 3.0: Unsaturated soil water and heat flow model. Theory, user manual, and examples. Pacific Northwest National Laboratory 13249.

Flerchinger, G.N., Hanson, C.L., Wight, J.R. (1996). Modeling evapotranspiration and surface energy budgets across a watershed. Water Resources Research 32: 2539-2548. https://doi.org/10.1029/96WR01240

Foster, S., Pulido-Bosch, A., Vallejos, Á., Molina, L., Llop, A., McDonal, A.M. (2018). Impact of irrigated agriculture on groundwater-recharge salinity: a major sustainability concern in semi-arid regions. Hydrogeology Journal 26: 2781-2791. https://doi.org/10.1007/s10040-018-1830-2

Gain, A.K., Giupponi, C., and Renaud, F.G. (2012). Climate change adaptation and vulnerability assessment of water resources systems in developing countries: a generalized framework and a feasibility study in Bangladesh. Water 4: 345–366. https://doi: 10.3390/w4020345

Gladnyeva, R., Saifadeen, A. (2012). Effects of hysteresis and temporal variability in meteorological input data in modeling of solute transport in unsaturated soil using HYDRUS-1D. Journal of Water Management and Research 68: 285-293. https://www.tidskriftenvatten.se/wp-content/uploads/2017/04/48_article_4604.pdf

Grine, R. (2009). Hydrogeological perspectives of the Hodnean basin. Master's thesis. USTHB, Algiers, Algeria. 140p.

Guiraud R, 1970. Geological map at 1:200,000 and notice of the Hodna basin. Edition FAO and MLARA, Algeria.

Gumiero, B.,Candonin, F., Boz, B., Da Borso, F., Colombani, N. (2019). Nitrogen Budget of Short Rotation Forests Amended with Digestate in Highly Permeable Soils. Applied Sciences 9: 4326. https://doi.org/10.3390/app9204326

Hansen, S., Jensen, H.E., Nielsen, N.E., Svendsen, H. (1990). NPo-research, A10: DAISY: soil plant atmosphere system model.

He, K., Yang, Y., Chen, S., Hu, Q., Liu, X., Gao, F. (2017). HYDRUS Simulation of Sustainable Brackish Water Irrigation in a Winter Wheat-Summer Maize Rotation System in the North China Plain. Water 9: 536. https://doi.org/10.3390/w9070536

Hopmans, J.W., Stricker, J.N.M. (1989). Stochastic analysis of soil water regime in a watershed. Journal of Hydrology 105: 57-84. https://doi.org/10.1016/0022-1694(89)90096-6

Jansson, P.E., Karlberg, L. (2001). Coupled heat and mass transfer model for soil-plant-atmosphere systems. Royal Institute of Technology. Department of Civil and Environmental Engineering, Stockholm.

Kanzari, S., Ben Nouna, B., Ben Mariem, S., Rezig, M. (2018). Hydrus-1D model calibration and validation in various field conditions for simulating water flow and salts transport in a semi-arid region of Tunisia. Sustainable Environment Research 28: 350-356. https://doi.org/10.1016/j.serj.2018.10.001

Khezzani, B., Bouchemal, S. (2018). Variations in groundwater levels and quality due to agricultural over-exploitation in an arid environment: the phreatic aquifer of the Souf oasis (Algerian Sahara). Environmental Earth Sciences 77(4): 142. https://doi.org/10.1007/s12665- 018- 7329-2

Leterme, B., Mallants, D., Jacques, D. (2012). Sensitivity of groundwater recharge using climatic analogs and HYDRUS-1D. Hydrology and Earth System Science 16: 2485-2497. https://doi.org/10.5194/hess-16-2485-2012

Li, B., Wang, Y., Hill, R.L., Li, Z. (2019). Effects of apple orchards converted from farmlands on soil water balance in the deep loess deposits based on HYDRUS-1D model. Agricultural, Ecosystems & Environment 285: 106645. https://doi.org/10.1016/j.agee.2019.106645

Ma, X., Bai, Y., Liu, X., & Wang, Y. (2023). Analysis of water infiltration characteristics and hydraulic parameters of sierozem soil under humic acid addition. Water (Switzerland) 15(10): 1915. https://doi.org/10.3390/w15101915

Madani, D. (2023). Study of the impacts of land degradation linked to desertification on the landscape and the socio-economic aspect in the M'Sila region, Eastern Algeria. PhD thesis, University of Biskra, Algeria. http://thesis.univ-biskra.dz

Mastrocicco, M., Gervasio, M.P., Busico, G., Colombani, N. (2021). Natural and anthropogenic factors driving groundwater resources salinization for agriculture use in the Campania plains (Southern Italy). Science of the Total Environment 758: 144033. https://doi.org/10.1016/j.scitotenv

Mualem, Y. (1976). A new model for predicting the hydraulic conductivity of unsaturated porous media. Water Resources Research 12: 513-522. https://doi.org/10.1029/WR012i003p00513

Ntona, M.M., Busico, G., Mastrocicco, M., Kazakis, N. (2022). Modeling groundwater and surface water interaction: An overview of current status and future challenges. Science of The Total Environment 846: 157355. https://doi.org/10.1016/j.scitotenv.2022.157355

Panda, B., Chidambaram, S., Nagappan, G., Thilagavathi, R., Kamaraj, P. (2020). Multiple thematic spatial integration technique to identify the groundwater recharge potential zones - A case study along the Courtallam region, Tamil Nadu, India. Arabian Journal of Geosciences 13(24): 1284. https://doi.org/10.1007/s12517-020-06223-8

Pruess, K. (1991). TOUGH2: A general-purpose numerical simulator for multiphase fluid and heat flow. Berkeley, California: Lawrence Berkeley Lab.

Pulido-Bosch, A., Rigol-Sanchez, J., Vallejos, A., Andreu, J.M., Ceron, J.C., Molina-Sanchez, L., Sola, F. (2018). Impacts of agricultural irrigation on groundwater salinity. Environmental Earth Sciences 77(5): 197. https://doi.org/10.1007/s12665-018-7386-6

Ramos, T.B., Darouich, H., Oliveira, A.R., Farzamian, M., Monteiro, T., Castanheira, N., Paz, A., Alexandre, C., Gonçalves, M.C., Pereira, L.S. (2023). Water use, soil water balance and soil salinization risks of Mediterranean tree orchards in southern Portugal under current climate variability: Issues for salinity control and irrigation management. Agricultural Water Management 283: 108319.   https://doi.org/10.1016/j.agwat.2023.108319

Razack, M., Jalludin, M., Gaba, A. H. (2019). Simulation of climate change impact on a coastal aquifer under arid climate. The Tadjourah Aquifer (Republic of Djibouti, Horn of Africa). Water 11: 2347. https://doi:10.3390/w11112347

Rawat, M., Sen, R., Onyekwelu, I., Wiederstein, T., Sharda, V. (2022). Modeling of groundwater nitrate contamination due to agricultural Activities - A systematic review. Water (Switzerland), 14(24): 4008. https://doi.org/10.3390/w14244008

Saâdi, M., Zghibi, A., Kanzari, S., 2018. Modeling interactions between saturated and unsaturated zones by Hydrus-1D in semi-arid regions (plain of Kairouan, Central Tunisia). Environment Monitoring Assessment 190: 170. https://doi.org/10.1007/s10661-018-6544-3

Salifu, M., Yidana, S.M., Anim-Gyampo, M., Appenteng, M., Saka, D., Aidoo, F., Gampson, E., Sarfo, M. (2017). Hydrochemical and isotopic studies of groundwater in the middle voltaian aquifers of the Gushegu district of the Northern region. Applied Water Science 7:1117–1129. https://doi.org/10.1007/s13201-015-0348-1

Scanlon, B.R., Healy, R.W., Cook, P.G. (2002). Choosing appropriate techniques for quantifying groundwater recharge. Hydrogeology Journal 10: 18-39. https://doi.org/10.1007/s10040-001-0176-2

Schaap, M.G., Leij, F.J., Van Genuchten, M.T., 2001. Rosetta: a computer program for estimating soil hydraulic parameters with hierarchical pedotransfer functions. Journal of Hydrology 251: 163-176. https://doi.org/10.1016/S0022-1694(01)00466-8

Selker, J.S., Duan, J., Parlange, J.Y.(1996). Green and Ampt infiltration into soils of variable pore size with depth. Water Resources Research 35: 1685-1688. https://doi.org/10.1029/1999WR900008

Šimůnek, J., Šejna, M., Saito, H., Sakai, M., Van Genuchten,M.T. (1998a). HYDRUS 1D software package for simulating the one-dimensional movement of water, heat, and multiple solutes in variably saturated media: IGWMC—TPS70 version 2.0. Colorado School of Mines.

Šimůnek, J., Šejna, M., Van Genuchten, M.T. (1998b). The HYDRUS-1D software package for simulating the one-dimensional movement of water, heat, and multiple solutes in variably saturated media, Version 2.0.

Šimůnek, J., Šejna, M., Van Genuchten, M.T. (2005). The Hydrus-1D Software Package for Simulating the One-dimensional Movement of Water, Heat, and Multiple Solutes in Variably-saturated Media; University of California-Riverside Research Reports: Riverside, CA, USA.

Šimůnek, J., Van Genuchten, M.T., Sejna, M. (2006). The HYDRUS Software Package for Simulating the Two and Three Dimensional Movement of Water, Heat, And Multiple Solutes in Variably Saturated Media. Technical Manual, Version 1.0, University of California.

Stephens, D.B. (1996). Vadose Zone Hydrology. Boca Raton, Florida: CRC Press.

Smerdon, B.D., Allen, D.M.,Neilsen, D. (2010). Evaluating the use of a gridded climate surface for modeling groundwater recharge in a semi-arid region (Okanagan Basin, Canada). Hydrological processes 24: 3087-3100. https://doi.org/10.1002/hyp.7724

Tafteh, R., Sepaskhah, A.R. (2012). Application of HYDRUS-1D model for simulating water and nitrate leaching from continuous and alternate furrow irrigated rapeseed and maize fields. Agricultural Water Management 113: 19-29.
    https://doi.org/10.1016/j.agwat.2012.06.011

Tarawneh, K., Ieyan, I., Alalwan, R., Sallam, S., Hammad, S. (2021). Assessment of heavy metals contamination levels in surfaces soil in Baqa'a area, Jordan. Jordan Journal of Earth and Environmental Sciences 12(4): 285-294.
https://jjees.hu.edu.jo/files/Vol12No4/JJEES_Vol_12_No_4_P2.pdf

Tomaz, A., Palma, P., Fialho, S., Lima, A., Alvarenga, P., Potes, M., Costa, M.J., Salgado, R. (2020). Risk assessment of irrigation-related soil salinization and sodification in Mediterranean areas. Water 12(12): 3569. https://doi.org/10.3390/w12123569

Van Dam, J.C., Huygen, J., Wesseling, J.G., Feddes, R.A., Kabat, P., Van Walsum, P.E.V., Van Diepen, C.A. (1997). Theory of SWAP version 2.0; Simulation of water flow, solute transport and plant growth in the soil-water-atmosphere-plant environment (N° 71, p. 167). DLO Winand Staring Center.

Van Genuchten, M.T. (1980). A closed-form equation for predicting the hydraulic, conductivity of unsaturated soils. Soil Science Society of America Journal 44: 892-898. https://doi.org/10.2136/sssaj1980.03615995004400050002x

Wang, X., Geng, X., Sadat-Noori, M., Zhang, Y. (2022). Groundwater-seawater exchange and environmental impacts. Frontiers in Water 4: 928615. https://doi: 10.3389/frwa.2022.928615

Zeng, W., Xu, C., Wu, J. Wang, J. (2014). Soil salt leaching under different irrigation regimes: HYDRUS-1D modeling and analysis. Journal of Arid Land 6: 44-58. https://doi.org/10.1007/s40333-013-0176-9

Xue, S., Ke, W., Zeng, J., Tabelin C.B., Xie, Y., Tang, L., Xiang, C., Jiang, J. (2023). Pollution prediction for heavy metals in soil-groundwater systems at smelting sites. Chemical Engineering Journal 473: 145499. https://doi.org/10.1016/j.cej.2023.145499